Inorganic Chemistry
Article

Inorg. Chem. **2009**, *48*, 8971–8976 **8971**
DOI: 10.1021/ic900134f

Carbon Dioxide Activation by "Non-nucleophilic" Lead Alkoxides

Eric C. Y. Tam, Nick C. Johnstone, Lorenzo Ferro, Peter B. Hitchcock, and J. Robin Fulton*

Department of Chemistry, University of Sussex, Falmer, Brighton BN1 9QJ, U.K.

Received January 21, 2009

A series of terminal lead alkoxides have been synthesized utilizing the bulky β-diketiminate ligand $[\{N(2,6\text{-}^{i}Pr_2C_6H_3)C(Me)\}_2CH]^-$ (BDI). The nucleophilicities of these alkoxides have been examined, and unexpected trends were observed. For instance, (BDI)PbOR reacts with methyl iodide only under forcing conditions yet reacts readily, but reversibly, with carbon dioxide. The degree of reversibility is strongly dependent upon minor changes in the R group. For instance, when R = isopropyl, the reversibility is only observed when the resulting alkyl carbonate is treated with other heterocumulenes; however, when R = *tert*-butyl, the reversibility is apparent upon any application of reduced pressure to the corresponding alkyl carbonate. The differences in the reversibility of carbon dioxide insertion are attributed to the ground-state energy differences of lead alkoxides. The mechanism of carbon dioxide insertion is discussed.

Introduction

In contrast to the well-documented reactivity of transition-metal alkoxides,[1−3] the chemistry of lead alkoxides has largely been ignored outside of gas-phase and theoretical studies.[4−6] Divalent lead has an aqueous acidity of 7.2, much smaller than that predicted based upon electrostatic parameters.[7] This acidity has been attributed to a more covalent Pb−O bond, in contrast to the highly polarized transition metal−oxygen bonds. In addition, lead's aqueous acidity has been used to justify its enhanced ability to cleave RNA. At biologically relevant pHs, there will be a sufficient amount of divalent lead hydroxide present to act as a base, deprotonating the 2′-hydroxyl proton of the RNA backbone, and a nucleophile in the cleavage of the resultant cyclic phosphate intermediate.[8,9] This implies that the Pb−O bond has some degree of polarity to be able to act as both a base and a nucleophile. However, no complementary chemical studies have been performed to back this hypothesis. As such, we set out to investigate the nature of the Pb−O bond in order to understand the degree of polarization of the bond. Herein, the results of such studies are reported, and our findings suggest that, although nucleophilic behavior with methyl iodide is not observed, lead alkoxides readily insert carbon dioxide into the Pb−O bond.

We have recently synthesized a series of monomeric divalent lead halides utilizing the bulky β-diketiminate anion $[\{N(2,6\text{-}^{i}Pr_2C_6H_3)C(Me)\}_2CH]^-$ (BDI) to stabilize the resulting three-coordinate lead complexes.[10] The chloride complex (BDI)PbCl (**1**) was used to synthesize monomeric lead aryloxide complexes in good yield.[11] Because metal aryloxide complexes are generally not as reactive as their alkoxide counterparts, for our reactivity studies, we turned our attention toward the synthesis of monomeric, terminal lead alkoxide complexes.

Results and Discussion

The treatment of a toluene solution of chloride **1** with $KO^{i}Pr$ or $KO^{t}Bu$ affords lead alkoxides (BDI)PbO^{i}Pr (**2**) and (BDI)PbO^{t}Bu (**3**), respectively (eq 1). Although these lead alkoxide complexes form a stable solid, they will slowly decompose in solution at ambient temperatures. The X-ray crystal structures were determined for both **2** and **3**, showing the expected pyramidal geometry of the ligands around the lead center (Figure 1).[10,11] Selected bond lengths and angles for alkoxides **2** and **3** are listed in Table 1, and data collection parameters are given in Table 2. Both alkyl groups of complexes **2** and **3** lie away from the BDI−Pb core; this is

*To whom correspondence should be addressed. E-mail: j.r.fulton@sussex.ac.uk.

(1) Bryndza, H. E.; Fong, L. K.; Paciello, R. A.; Tam, W.; Bercaw, J. E. *J. Am. Chem. Soc.* **1987**, *109*, 1444.
(2) Bryndza, H. E.; Tam, W. *Chem. Rev.* **1988**, *88*, 1163.
(3) Fulton, J. R.; Holland, A. W.; Fox, D. J.; Bergman, R. G. *Acc. Chem. Res.* **2002**, *35*, 44.
(4) Akibo-Betts, G.; Barran, P. E.; Puskar, L.; Duncombe, B.; Cox, H.; Stace, A. J. *J. Am. Chem. Soc.* **2002**, *124*, 9257.
(5) Cox, H.; Stace, A. J. *J. Am. Chem. Soc.* **2004**, *126*, 3939.
(6) Stace, A. J. *J. Phys. Chem. A* **2002**, *106*, 7993.
(7) Burgess, J. *Metal Ions in Solution*; Ellis Horwood Ltd.: Chichester, U.K., 1978.
(8) Barciszewska, M. Z.; Szymanski, M.; Wyszko, E.; Pas, J.; Rychlewski, L.; Barciszewski, J. *Mutat. Res.* **2005**, *589*, 103.
(9) Winter, D.; Polacek, N.; Halama, E.; Streicher, B.; Barta, A. *Nucleic Acids Res.* **1997**, *25*, 1817.
(10) Chen, M.; Fulton, J. R.; Hitchcock, P. B.; Johnstone, N. C.; Lappert, M. F.; Protchenko, A. V. *Dalton Trans.* **2007**, 2770.
(11) Fulton, J. R.; Hitchcock, P. B.; Johnstone, N. C.; Tam, E. C. Y. *Dalton Trans.* **2007**, 3360.

Published on Web 08/21/2009

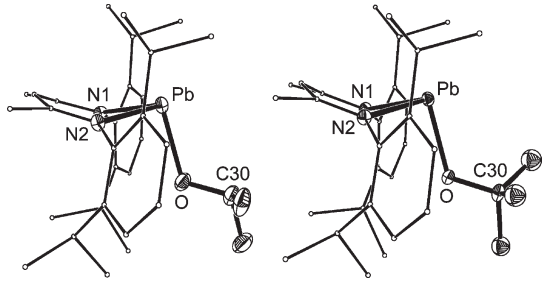

Figure 1. ORTEP diagram of lead isopropoxide **2** (left) and lead *tert*-butoxide **3** (right), with H atoms omitted and BDI C atoms minimized for clarity. The ellipsoid probability is shown at 30%.

Table 1. Selected Bond Lengths and Angles for Compounds **2** and **3**

	LPbO^{i}Pr (**2**)	LPbO^{t}Bu (**3**)
Pb−O	2.135(3)	2.126(3)
Pb−N1	2.307(3)	2.317(3)
Pb−N2	2.311(3)	2.299(3)
O−C30	1.413(5)	1.415(4)
N1−Pb−N2	80.56(9)	81.04(10)
N1−Pb−O	94.94(10)	92.74(10)
N2−Pb−O	93.49(10)	92.26(10)
Pb−O−C30	118.0(2)	121.4(2)
sum of the angles around Pb	268.99	266.04
DOP[a] (%)	101	104

[a] Degree of pyramidalization (DOP) = [360 − (sum of the angles)/0.9].[20]

in contrast to the isostructural tin system, in which the alkyl group lies below the plane consisting of N1−Pb−N2.[12]

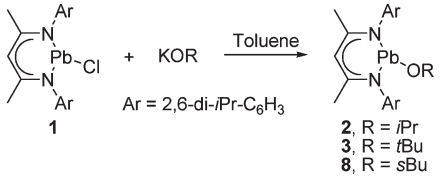

(1)

Two different types of lead alkoxide reactivities were investigated: basicity and nucleophilicity. The treatment of alkoxides **2** or **3** with 2,4-di-*tert*-butylphenol results in alcohol exchange reactions to form the known (BDI)Pb−OAr (Ar = 2,4-^{t}Bu$_2$C$_6$H$_3$) complex **4** with elimination of the corresponding aliphatic alcohols. This reactivity is similar to that observed in late-transition-metal alkoxide systems. However, the presence of free alcohol results in decomposition of aryloxide **4** to an insoluble white precipitate and protonated BDI. Potentially because of their higher pK_a, carbo acids are not reactive toward **2** and **3**; the treatment of isopropoxide **2** with fluorene did not yield the fluorenide anion, and the addition of 1,4-cyclohexadiene did not result in dimerization to an equilibrium mixture of 1,4- and 1,2-cyclohexadiene.

Both lead alkoxides **2** and **3** display seemingly contradictory reactivities toward electrophiles. For instance, neither reacts with benzyl bromide. When methyl iodide was added to either **2** or **3**, the formation of lead iodide was only observed after 2 days at 60 °C.[10] In sharp contrast, both alkoxides react readily with CO_2 (eq 2). The treatment of isopropoxide **2** with 1 equiv of CO_2 results in the clean and quantitative conversion to lead alkyl carbonate **5** after 30 min at room temperature. The IR spectrum shows a stretch at 1695 cm^{-1} (CCl_4), indicative of a carbonate carbonyl functionality; this is further supported by a

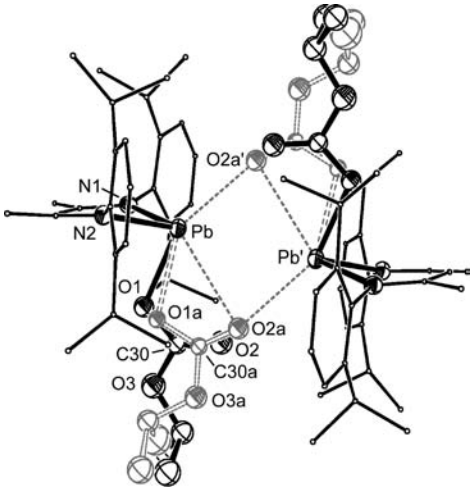

Figure 2. ORTEP diagram of lead carbonate **5** showing both components of the unit cell (major = black; minor = gray). H atoms are omitted and BDI C atoms minimized for clarity. Atoms with a prime are at equivalent positions ($-x$, $-y$, $-z$).

^{13}C NMR spectral resonance at 160.9 ppm. Crystals suitable for an X-ray diffraction study were grown at −30 °C in toluene. Two different binding modes for lead carbonate were observed in the solid state (Figure 2; see Table 3 for selected bond lengths and angles). In the major component, the carbonate is bound in an η^1 fashion and there is weak, long-distance interaction between O2 and Pb′. In the minor component, the carbonate is bound in an η^2 fashion and there is a shorter distance between O2a and Pb′, indicative of a stronger interaction between the two lead carbonate molecules.

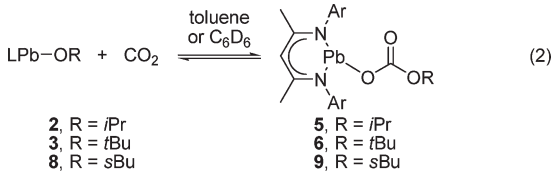

(2)

Because insertion of CO_2 into transition-metal alkoxides can be reversible,[13] we investigated whether the same was true for carbonate **5**. Although the formation of isopropoxide **2** is not observed when **5** is subjected to reduced pressure, the addition of $^{13}CO_2$ to the carbonate does result in ^{13}C incorporation into **5**.

Lead *tert*-butoxide **3** also reacts readily with CO_2 to form lead carbonate **6** (IR: 1699 cm^{-1}, CCl_4). In contrast to the isopropoxide system, the reaction is markedly reversible: the application of reduced pressure results in the almost quantitative formation of alkoxide **3**, thwarting attempts to characterize **6** in the solid state.

Pronounced differences in the reactivity of isopropoxide **2** and *tert*-butoxide **3** were observed upon treatment with phenyl isocyanate. With the former, insertion into the Pb−O bond to generate lead carbamate **7** is observed after 1 day at room temperature (eq 3). X-ray crystallography confirmed the presence of a Pb−N carbamate bond (Figure 3), with the *N*-phenyl group lying perpendicular to and below the plane consisting of N1−Pb−N2. Selected bond lengths and angles are listed in Table 4. In contrast, with *tert*-butoxide **3**, an

(12) Dove, A. P.; Gibson, V. C.; Marshall, E. L.; Rzepa, H. S.; White, A. J. P.; Williams, D. J. *J. Am. Chem. Soc.* **2006**, *128*, 9834.

(13) For example, see: Tsuda, T.; Saegusa, T. *Inorg. Chem.* **1972**, *11*, 2561. Simpson, R. D.; Bergman, R. G. *Organometallics* **1992**, *11*, 4306. Mandal, S. K.; Ho, D. M.; Orchin, M. *Organometallics* **1993**, *12*, 1714.

Table 2. Crystallographic Data for Compounds **2**, **3**, **5**, and **7**

	LPbO^{i}Pr (**2**)	LPbO^{t}Bu (**3**)	LPbOCO$_2{}^i$Pr (**5**)[a]	LPb[N(Ph)C(O)O^{i}Pr (**7**)[b]
chemical formula	$C_{32}H_{48}N_2OPb$	$C_{33}H_{50}N_2OPb$	$C_{33}H_{48}N_2O_3Pb\cdot0.5(C_7H_8)$	$C_{44}H_{65}N_3O_2Pb$
fw	683.91	697.94	773.99	875.18
temperature (K)	172(2)	173(2)	173(2)	173(2)
wavelength (Å)	0.710 73	0.710 70	0.710 73	0.710 73
cryst size (mm^3)	0.20 × 0.20 × 0.15	0.25 × 0.20 × 0.10	0.15 × 0.10 × 0.05	0.15 × 0.15 × 0.1
cryst syst	triclinic	monoclinic	triclinic	triclinic
space group	$P\bar{1}$ (No. 2)	$P2_1/n$ (No. 14)	$P\bar{1}$ (No. 2)	$P\bar{1}$ (No. 2)
a (Å)	8.6979(2)	13.3743(1)	11.9673(4)	11.5616(3)
b (Å)	12.1195(3)	16.8363(2)	13.2339(5)	11.6261(3)
c (Å)	15.1146(3)	15.2434(2)	13.5828(3)	18.2619(4)
α (deg)	92.885(1)	90	99.649(2)	102.146(1)
β (deg)	98.639(1)	108.168(1)	106.996(2)	95.723(2)
γ (deg)	97.444(1)	90	113.105(1)	112.814(1)
V (Å^3)	1559.71(6)	3261.29(6)	1792.09(10)	2166.78(9)
Z	2	4	2	2
p_c (Mg m^{-3})	1.46	1.42	1.43	1.34
abs coeff (mm^{-1})	5.43	5.20	4.74	3.93
θ range for data collection (deg)	3.40−26.02	3.43−25.82	3.47−26.02	3.44−26.01
measd/indep reflns/R(int)	23 519/6112/0.044	41 847/6251/0.061	26 307/7017/0.066	23 224/8472/ 0.054
reflns with $I > 2\sigma(I)$	5783	5497	5851	7159
data/restraints/param	6112/0/337	6251/30/334	7017/34/380	8472/7/438
GOF on F^2	0.826	1.051	0.962	1.027
final R indices [$I > 2\sigma(I)$]	R1 = 0.023, wR2 = 0.059	R1 = 0.027, wR2 = 0.064	R1 = 0.047, wR2 = 0.107	R1 = 0.041, wR2 = 0.083
R indices (all data)	R1 = 0.026, wR2 = 0.061	R1 = 0.033, wR2 = 0.067	R1 = 0.0631, wR2 = 0.11571	R1 = 0.057, wR2 = 0.090
largst diff peak and hole (e Å^3)	0.78 and −1.37	1.37 and −1.40 (near Pb)	2.45 and −0.72 (close to Pb)	0.96 and 1.40

[a] The OC(O)O^{i}Pr group is disordered unequally over two arrangements with only some of the atoms resolved. The positions for the major component could be located, and for the minor component, approximate starting positions were estimated. The two orientations were then restrained to have similar geometry by use of the *same* instruction. This refinement converged successfully. There is a molecule of toluene solvate disordered about an inversion center for which the H atoms were omitted. All disordered atoms were left isotropic. [b] The poorly defined pentane solvate was included with isotropic C atoms and restrained geometry.

intractable reaction mixture is found. Even though the reaction between isopropoxide **2** and CO_2 is much faster than the reaction between **2** and phenyl isocyanate, there is a thermodynamic preference for the latter; the treatment of alkyl carbonate **5** with phenyl isocyanate results in an exclusive conversion to carbamate **7**. Neither alkoxide reacts with dicyclohexylcarbodiimide, even at elevated temperatures. Both alkoxides **2** and **3**, and their corresponding alkyl carbonates **5** and **6**, react with CS_2 to give intractable reaction mixtures.

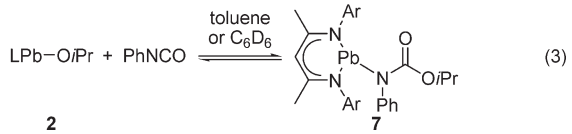

2 **7** (3)

To further understand the differences observed in the reactivity between isopropoxide **2** and *tert*-butoxide **3**, we synthesized the *sec*-butoxide complex **8**. The treatment of *sec*-butoxide **8** with CO_2 resulted in the expected formation of the corresponding carbonate **9** (IR: 1645 cm^{-1}, CCl_4). The degree of reversibility of this reaction is intermediate between the isopropoxide and *tert*-butoxide systems. For instance, when a vacuum is applied for 10 min to an NMR-scale solution of *tert*-butoxide carbonate **6**, almost complete reversion to alkoxide **3** is observed; however, when a similar procedure is repeated for a solution of *sec*-butoxide carbonate **9**, only 20% reversion to alkoxide **8** is observed. Unfortunately, as in the *tert*-butoxide case, this reversibility has prevented solid-state characterization of *sec*-butoxide carbonate **9**. Interestingly, solutions of both the isopropoxide carbonate **4** and *sec*-butoxide carbonate **9** are thermally stable to 60 °C, whereas the *tert*-butoxide carbonate **5** decomposes after standing at room temperature overnight.

The noticeable difference in reactivity with respect to deinsertion of CO_2 from carbonates **5**, **6**, and **9** can be attributed to the ground-state energy differences of the alkoxides. The stability of transition-metal alkoxides correlates to the pK_a of the corresponding alcohol; that is, the higher the pK_a, the more stable the metal alkoxide.[1] If a similar trend is assumed for lead alkoxides, then the lead isopropoxide **2** is less stable than the lead *tert*-butoxide **3** (pK_a of isopropyl alcohol is 30.2, whereas the pK_a of *tert*-butanol is 2 pK_a units higher).[14] The alkyl group will have a much smaller effect on the pK_a of the corresponding alkyl carbonates. An attempt was made to determine the rate of $^{13}CO_2$ exchange with each of the carbonates using ^{13}C NMR spectroscopy. Although exchange was observed, we were unable to obtain reproducible rate data. As such, we investigated the relative ground-state differences between the reactants and products using the B3LYP density functional theory and LanL2DZ pseudopotentials (and basis set) implemented in *Gaussian 03*.[15] The $\Delta H°$ value for the insertion of CO_2 into lead isopropoxide **2** was slightly greater than the analogous reaction for both the lead *sec*-butoxide **8** and

(14) Olmstead, W. M.; Margolin, Z.; Bordwell, F. G. *J. Org. Chem.* **1980**, *45*, 3295.

(15) Frisch, M. J.; Trucks, G. W.; Schlegel, H. B.; Scuseria, G. E.; Robb, M. A.; Cheeseman, J. R.; Montgomery, J. A., Jr.; Vreven, T.; Kudin, K. N.; Burant, J. C.; Millam, J. M.; Iyengar, S. S.; Tomasi, J.; Barone, V.; Mennucci, B.; Cossi, M.; Scalmani, G.; Rega, N.; Petersson, G. A.; Nakatsuji, H.; Hada, M.; Ehara, M.; Toyota, K.; Fukuda, R.; Hasegawa, J.; Ishida, M.; Nakajima, T.; honda, Y.; Kitao, O.; Nakai, H.; Klene, M.; Li, X.; Knox, J. E.; Hratchian, H. P.; Cross, J. B.; Adamo, C.; Jaramillo, J.; Gomperts, R.; Stratmann, R. E.; Yazyev, O.; Austin, A. J.; Cammi, R.; Pomelli, C.; Ochterski, J. W.; Ayala, P. Y.; Morokuma, K.; Voth, G. A.; Salvador, P.; Dannenberg, J. J.; Zakrzewski, V. G.; Dapprich, S.; Daniels, A. D.; Strain, M. C.; Farkas, O.; Malick, D. K.; Rabuck, A. D.; Raghavachari, K.; Foresman, J. B.; Ortiz, J. V.; Cuiq, Q.; Baboul, A. G.; Clifford, S.; Cioslowski, J.; Stefanov, B. B.; Liu, G.; Liashenko, A.; Piskorz, P.; Komaromi, I.; Martin, R. L.; Fox, D. J.; Keith, T.; Al-Laham, M. A.; Peng, C. Y.; Nanayakkara, A.; Challacombe, M.; Pople, J. A. *Gaussian 03*, revision C.02; Gaussian Inc.: Wallingford, CT, **2004**.

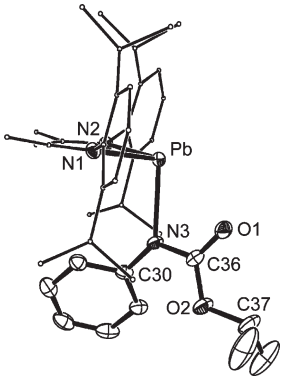

Figure 3. ORTEP diagram of lead carbamate **7** with H atoms omitted and BDI C atoms minimized for clarity. The ellipsoid probability is shown at 30%.

Table 3. Selected Bond Lengths and Angles for Compound **5**

Pb−O1	2.217(10)	N1−Pb−N2	83.23(18)
Pb−N1	2.292(5)	N1−Pb−O1	83.5(3)
Pb−N2	2.291(5)	N2−Pb−O1	82.2(3)
Pb−O1A	2.399(13)	N1−Pb−O1A	91.7(3)
Pb−O2A′	2.777(13)	N2−Pb−O1A	90.2(3)
Pb···Pb′	3.7842(5)	O1−Pb−O2A′	145.7(4)
O1−C30	1.309(16)	N1−Pb−O2A′	130.5(3)
O2−C30	1.188(17)	N2−Pb−O2A′	96.3(3)
O3−C30	1.372(14)	O1A−Pb−O2A′	137.8(4)
O3−C31	1.451(15)	Pb−O1−C30	113.5(8)
O1A−C30A	1.314(18)	O1−C30−O2	127.9(12)
O2A−C30A	1.18(2)	O1−C30−O3	107.9(12)
O3A−C30A	1.355(15)	O2−C30−O3	124.1(13)
O3A−C31A	1.453(16)	Pb−O1A−C30A	106.2(9)
		Pb′−O2A−C30A	148.4(11)
		O1A−C30−O2A	125.1(13)
sum of the angles around Pb	266.04	O1A−C30−O3A	114.9(16)
DOP[a] (%)	104	O2A−C30−O3A	119.8(16)

[a] Degree of pyramidalization (DOP) = [360 − (sum of the angles)/0.9].[20]

Table 4. Selected Bond Lengths and Angles for Compound **7**

Pb−N1	2.335(4)	N1−Pb−N2	82.47(14)
Pb−N2	2.321(4)	N1−Pb−N3	95.94(14)
Pb−N3	2.340(4)	N2−Pb−N3	96.84(14)
N3−C30	1.420(6)	Pb−N3−C30	132.5(3)
N3−C36	1.340(6)	Pb−N3−C36	103.2(3)
C36−O1	1.236(6)	N3−C36−O1	121.8(5)
C36−O2	1.348(6)	N3−C36−O2	116.4(5)
O2−C37	1.466(7)	O1−C36−O2	121.7(5)
		C36−O2−C37	116.9(4)
		sum of the angles around Pb	275.25
		DOP[a]	94%

[a] Degree of pyramidalization (DOP) = [360 − (sum of the angles)/0.9].[20]

tert-butoxide **3** cases (−9.4 kcal mol^{-1} vs −8.9 and −8.4 kcal mol^{-1}, respectively). Although these are gas-phase calculations, it is reassuring that the trends observed are similar to our experimental results.

The slow to nonexistent reactivity of our lead alkoxides with aliphatic electrophiles is in sharp contrast to the reactivity observed with transition-metal alkoxides. The most striking difference is with Vahrenkamp's pyrazolborate−zinc methoxide complex ($Tp^{Ph,Me}$Zn-OMe),[16] which reacts readily with methyl iodide to generate the corresponding dimethyl ether and pyrazolborate−zinc iodide complex, yet only reacts with CO_2 under forced conditions and not at all with phenyl isocyanate. This implies that the lead alkoxides lack nucleophilic characteristics. Space-filling models of alkoxide **2** reveal that the O atom lies inside a pocket surrounded by the BDI isopropyl groups and the alkyl group on the O atom. Thus, we cannot conclusively state that our lead alkoxides are non-nucleophilic because of potential steric arguments. However, we can conclude that a nucleophilic O atom is *not available* for reactivity.

The mechanism of CO_2 insertion into transition-metal alkoxides is generally thought to proceed via a concerted process in which the new carbon−oxygen and metal−carbonate bonds form at the same time as the cleavage of the metal−alkoxide bond.[17] The symmetry of this transition state must vary depending upon the nucleophilicity of the O atom and the propensity for CO_2 to bind to the metal center. In our examples, the lack of an available nucleophilic O atom implies that coordination of CO_2 to the metal center is key, and it must be this coordination that induces the alkoxide to react with CO_2. This can occur either by changing the steric environment around the alkoxide or by shifting the electron density such that the alkoxide ligand becomes more nucleophilic and CO_2 becomes more electrophilic. However, we have been unable to observe the binding of additional ligands to the metal center, nor can we gain evidence for binding using computational analysis. The addition of extraneous ligands such as CH_3CN, THF, TMEDA, and N-heterocyclic carbenes as well as softer ligands such as trimethyl- and triphenylphosphine did not result in either measurable inhibition of CO_2 insertion or strong evidence of coordination. Indeed, crystals of the alkoxides **2**, **3**, or **8** grown in a 50:50 mixture of CH_3CN and hexane did not result in coordinated CH_3CN in the solid state.

The differing reactivity between our lead alkoxides and transition-metal alkoxides is intriguing both from a fundamental viewpoint and from implications in the mechanism of lead-mediated RNA cleavage, and we are testing whether our apparent non-nucleophilic behavior can be reproduced with less sterically hindered lead alkoxides. In addition, we are currently investigating the mechanism of CO_2 insertion using kinetic studies on the slower isostructural tin system.[12]

Experimental Section

All manipulations were carried out in an atmosphere of dry nitrogen or argon using standard Schlenk techniques or in an inert-atmosphere glovebox. Solvents were dried from the appropriate drying agent, distilled, degassed, and stored over 4 Å sieves. (BDI)PbCl (**1**) was prepared according to the literature.[10] Potassium alkoxide salts were prepared by the slow addition of the relevant alcohol (dried and distilled) to a suspension of potassium hydride. Phenyl isocyanate and carbon disulfide were freshly dried and distilled before use. Carbon dioxide was used as received (Union Carbide, 99.999%), and $^{13}CO_2$ was 99 atom %. The ^{1}H and ^{13}C NMR spectra were recorded on a Bruker DPX 300 MHz spectrometer, a Varian 400 MHz spectrometer, or a Varian 500 MHz spectrometer. The ^{1}H and ^{13}C NMR spectroscopy chemical shifts are given relative to residual solvent peaks,

(16) Brombacher, H.; Vahrenkamp, H. *Inorg. Chem.* **2004**, *43*, 6042.

(17) For a few examples, see ref 15 as well as the following: Chisholm, M. H.; Cotton, F. A.; Extine, M. W.; Reichert, W. W. *J. Am. Chem. Soc.* **1978**, *100*, 1727. Darensbourg, D. J.; Sanchez, K. M.; Rheingold, A. L. *J. Am. Chem. Soc.* **1987**, *109*, 290. Campora, J.; Matas, I.; Palma, P.; Alvarez, E.; Graiff, C.; Tiripicchio, A. *Organometallics* **2007**, *26*, 3840.

and the ^{207}Pb elements were externally referenced to $PbMe_4$. The data for the X-ray structures were collected at 173 K on a Nonius Kappa CCD diffractometer, k(Mo Kα) = 0.710 73 Å and refined using the *SHELXL-97* software package.[18]

[CH{(CH$_3$)$_2$CN-2,6-^{i}Pr$_2$C$_6$H$_3$}$_2$PbO^{i}Pr] (2). 1 (1.08 g, 1.64 mmol) was added to a stirred suspension of KO^{i}Pr (0.127 g, 1.64 mmol) in 10 mL of toluene at room temperature. The reaction vessel was wrapped in foil, and the mixture was stirred overnight. The mixture was filtered through a pad of Celite, and the solvent was removed in a vacuum. The resulting brown oil was dissolved in a minimum of pentane and **2** crystallized upon standing at −30 °C overnight (0.686 g, 62%). ^{1}H NMR (C_6D_6, 293 K): δ 7.26 (d, 2H, J = 7.5 Hz, *m*-H), 7.20 (t, 2H, J = 7.5 Hz, *p*-H), 7.09 (d, 2H, J = 7.5 Hz, *m*-H), 4.96 (septet, 1H, J = 6.8 Hz, C*H*Me$_2$), 4.71 (s, 1H, middle CH), 3.95 (septet, 2H, J = 6.8 Hz, C*H*Me$_2$), 3.18 (septet, 2H, J = 6.8 Hz, C*H*Me$_2$), 1.69 (s, 6H, NC*Me*), 1.57 (d, 6H, J = 6.7 Hz, CH*Me*$_2$), 1.29 (d, 6H, J = 6.8 Hz, CH*Me*$_2$), 1.20 (d, 6H, J = 6.9 Hz, CH*Me*$_2$), 1.17 (d, 6H, J = 6.8 Hz, CH*Me*$_2$), 1.07 (d, 6H, J = 5.9 Hz, CH*Me*$_2$). ^{13}C{^{1}H} NMR (C_6D_6, 293 K): δ 163.9 (N*C*Me), 145.1 and 143.3 (*ipso*- and *o*-C of Ar), 126.4, 124.8, and 123.9 (*m*- and *p*-CH of Ar), 100.2 (middle CH), 66.0 (O*C*HMe$_2$), 30.6 (NC*Me*), 28.2 (OCH*Me*$_2$), 26.3, 25.7, 24.9, and 24.6 (CH*Me*$_2$). IR (Nujol, ν/cm^{-1}): 1553 (s), 1512 (s), 1317 (s), 1265 (s), 1172 (s), 1117 (s), 1012 (s), 960 (s),790 (s), 752 (s), 722 (s). Anal. Calcd for $C_{32}H_{48}ON_2Pb$: C, 56.20; H, 7.07; N, 4.10. Found: C, 56.30; H, 7.17; N, 4.13.

[CH{(CH$_3$)$_2$CN-2,6-^{i}Pr$_2$C$_6$H$_3$}$_2$PbO^{t}Bu] (3). 1 (0.908 g, 1.38 mmol) was added to a stirred suspension of KO^{t}Bu (0.154 g, 1.38 mmol) in toluene (15 mL) at room temperature, and the mixture was stirred overnight. The reaction mixture was filtered through Celite. The solvent was removed under vacuum, producing an orange solid as the crude product. The crude product was washed with pentane and recrystallized from toluene overnight, yielding yellow light-sensitive crystals of **3** (0.720 g, 75%). ^{1}H NMR (300 MHz, C_6D_6, 293 K): δ 7.26 (dd, 2H, J = 7.5 Hz, Ar*H*), 7.10 (d, 2H, J = 7.5 Hz, Ar*H*), 7.04 (dd, 2H, J = 7.5 Hz, Ar*H*), 4.57 (s, 1H, middle C*H*), 3.83 (septet, 2H, J = 6.8 Hz, C*H*Me$_2$), 3.12 (septet, 2H, J = 6.8 Hz, C*H*Me$_2$), 1.65 (s, 6H, CC*H*$_3$), 1.63 (d, 6H, J = 6.8 Hz, C(C*H*$_3$)$_2$), 1.25 (d, 6H, J = 6.9 Hz, C(C*H*$_3$)$_2$), 1.19 (d, 6H, J = 6.9 Hz, C(C*H*$_3$)$_2$), 1.14 (d, 6H, J = 6.8 Hz, C(C*H*$_3$)$_2$), 0.88 (s, 9H, C(C*H*$_3$)$_3$). ^{13}C{^{1}H} NMR (300 MHz, C_6D_6, 293 K): 164.0 (N*C*Me), 145.1 (*ipso*-*C*), 142.8 (*o*-*C*), 141.5 (*o*-*C*), 126.0 (*p*-*C*), 123.7 (*m*-*C*), 123.6 (*m*-*C*), 98.0 (middle *C*H), 69.1 (O*C*Me$_3$), 36.7 (OC(*C*H$_3$)$_3$), 28.4 (*C*HMe$_2$), 28.0 (*C*HMe$_2$), 26.1 (NC*C*H$_3$), 25.2 (C(*C*H$_3$)$_2$), 24.8 (C(*C*H$_3$)$_2$), 24.6 (C(*C*H$_3$)$_2$), 23.9 (C(*C*H$_3$)$_2$). IR (Nujol, ν/cm^{-1}): 1556 (s), 1511 (s), 1318 (s), 1262 (s), 1227 (s), 1015 (s), 941 (s), 838 (s), 791 (s), 751 (s). Anal. Calcd for $C_{33}H_{50}N_2OPb$: C, 56.79; H, 7.22; N, 4.01. Found: C, 56.70; H, 7.15; N, 3.97.

[CH{(CH$_3$)$_2$CN-2,6-^{i}Pr$_2$C$_6$H$_3$}$_2$Pb(CO$_2$)O^{i}Pr] (5). 2 was dissolved in toluene (2 mL) and loaded into an ampule wrapped in aluminum foil. The reaction vessel was connected to a Schlenk line and a cylinder of high-purity CO_2. The vessel was submerged in a dry ice/acetone bath, and after three pump/refill cycles, CO_2 was introduced at a pressure of 1.5 bar. Thawing followed by removal of the solvent gave **5** as a yellow solid in quantitative yield. ^{1}H NMR (C_6D_6, 300 K): δ 7.19 (s, 6H, Ar*H*), 4.97 (septet, 1H, J = 6.3 Hz, OC*H*Me$_2$), 4.86 (s, 1H, middle CH), 3.39−3.32 (br multiplet, 4H), 3.02 (septet, 2H, J = 6.9 Hz, C*H*Me$_2$), 1.69 (s, 6H, NC*Me*), 1.30 (d, 12H, J = 6.3 Hz, CH*Me*$_2$), 1.20 (d, 12H, J = 6.3 Hz, CH*Me*$_2$), 1.24 (d, 6H, J = 6.8 Hz, OCH*Me*$_2$). ^{13}C{^{1}H} NMR (500 MHz, toluene-d_8, 303 K): δ 164.1 (N*C*Me), 160.9 (O*C*=O), 142.8 (*ipso*-*C*), 129.2 (*o*-*C*), 128.3 (*o*-*C*), 127.0 (*p*-*C*), 125.4 (*m*-*C*), 124.5 (*m*-*C*), 103.6 (middle *C*H), 68.7 (O*C*(CH$_3$)$_2$), 34.6 (OC(*C*H$_3$)$_2$), 28.3 (*C*HMe$_2$), 26.0 (*C*HMe$_2$), 24.7 (NC*C*H$_3$), 24.5 (CH(*C*H$_3$)$_2$), 22.8 (CH(*C*H$_3$)$_2$), 22.7 (CH(*C*H$_3$)$_2$), 14.3 (CH(*C*H$_3$)$_2$). ^{207}Pb NMR (400 MHz, toluene-d_8, 303 K): δ 808.7. IR (Nujol, ν/cm^{-1}): 3056 (s), 1611 (s), 1583 (s), 1551 (s), 1519 (s), 1317 (s), 1294 (s), 1171 (s), 1108 (s), 1055 (s), 1020 (s). IR (CCl_4, ν/cm^{-1}): 3060 (s), 2963(s), 2928 (s), 2871 (s), 2335 (br), 1699 (s), 1463 (s), 1438 (s), 1387 (br), 1319 (s), 1292 (s), 1173 (s), 1115 (s). Anal. Calcd for $C_{33}H_{48}N_2O_3Pb$: C, 54.45; H, 6.65; N, 3.85. Found: C, 54.49; H, 6.71; N, 3.75.

[CH{(CH$_3$)$_2$CN-2,6-^{i}Pr$_2$C$_6$H$_3$}$_2$Pb(CO$_2$)O^{t}Bu] (6). 3 (0.050 g, 0.072 mmol) was dissolved in toluene-d_8 in an NMR tube sealed with a Young's tap. The gas inside the NMR tube was evacuated. CO_2 (0.0047 mg, 0.109 mmol) was then added. A yellow solution mixture was observed, and the reaction mixture was kept at room temperature for 24 h and was monitored by ^{1}H NMR spectroscopy. ^{1}H NMR (400 MHz, toluene-d_8, 203 K): δ 7.15 (s, 2H, Ar*H*), 7.07 (d, 2H, J = 4 Hz, Ar*H*), 6.95 (d, 2H, J = 8 Hz, Ar*H*), 4.79 (s, 1H, middle C*H*), 3.64 (m, 2H, C*H*Me$_2$), 2.94 (m, 2H, C*H*Me$_2$), 1.62 (s, 6H, CC*H*$_3$), 1.58 (br, 6H, J = 4 Hz, C(C*H*$_3$)$_2$), 1.50 (d, 6H, J = 4 Hz, C(C*H*$_3$)$_2$), 1.17 (d, 6H, J = 4 Hz, C(C*H*$_3$)$_2$), 1.08 (s, 9H, C(C*H*$_3$)$_3$). ^{13}C{^{1}H} NMR (400 MHz, toluene-d_8, 203 K): δ 163.5 (N*C*Me), 160.3 (O*C*O), 144.2 (*ipso*-*C*), 142.3 (*o*-*C*), 141.6 (*o*-*C*), 103.5 (middle *C*H), 76.6 (O*C*HMe$_2$), 28.5 (OCH(*C*H$_3$)$_2$), 28.1 (NC*C*H$_3$), 27.6 (*C*HMe$_2$), 27.4 (*C*HMe$_2$), 26.8 (*C*HMe$_2$), 26.5 (*C*HMe$_2$), 25.0 (C(*C*H$_3$)$_2$), 24.7 (C(*C*H$_3$)$_2$), 24.3 (C(*C*H$_3$)$_2$), 24.1 (C(*C*H$_3$)$_2$). ^{207}Pb NMR (400 MHz, toluene-d_8, 303 K): δ 817.4. IR (CCl_4, ν/cm^{-1}): 3060 (s), 2965 (s), 2928 (s), 2869 (s), 1699 (s), 1463 (s), 1438 (s), 1389 (b), 1366 (b), 1172 (s), 1102 (s).

[CH{(CH$_3$)$_2$CN-2,6-^{i}Pr$_2$C$_6$H$_3$}$_2$Pb(N(Ph)CO)O^{i}Pr] (7).[19] Phenyl isocyanate (0.032 mL, 0.294 mmol) was added to a solution of **2** (0.196 g, 0.287 mmol) in toluene (3 mL). The reaction vessel was wrapped in foil and stirred at room temperature for 3 h. The volatiles were removed, and the resulting orange residue was dissolved in a minimum of pentane. **7** crystallized upon standing at −30 °C overnight (0.100 g, 44%). ^{1}H NMR (500 MHz, toluene-d_8, 303 K): δ 7.59 (br, 2H, ArH), 7.27 (t, 2H, J = 15 Hz, ArH), 6.85 (t, 1H, J = 15 Hz, ArH), 5.03 (s, 1H, middle C*H*), 4.91 (br, 1H, OC*H*Me$_2$), 3.13 (br, 4H, C*H*Me$_2$), 1.67 (s, 6H, CC*H*$_3$), 1.28 (d, 1H, J = 5 Hz, C(C*H*$_3$)$_2$), 1.25 (d, 1H, J = 5 Hz, C(C*H*$_3$)$_2$), 1.15 (2H, br d, J = 10 Hz, C(C*H*$_3$)$_2$), 0.98 (6H, br, C(C*H*$_3$)$_2$), 0.88 (d, 2H, J = 10 Hz, C(C*H*$_3$)$_2$), 0.87 (d, 2H, J = 5 Hz, OC(C*H*$_3$)$_2$). ^{13}C{^{1}H} NMR (500 MHz, toluene-d_8, 303 K): δ 165.0, 143.3, 129.2, 128.3, 127.9, 126.8, 126.0, 121.7, 103.2, 67.2, 34.6, 28.2, 25.5, 25.2, 24.6, 22.8, 22.4, 14.3. ^{13}C{^{1}H} NMR (400 MHz, toluene-d_8, 198 K): δ 164.7, 164.0, 163.7, 161.4, 158.9, 147.7, 146.6, 144.6, 144.1, 142.9, 142.4, 141.7, 141.4, 129.7, 127.3, 126.5, 126.0, 125.4, 68.0, 67.1, 66.8, 66.4, 65.8, 65.3, 34.5, 27.2, 26.7, 25.8, 25.0, 24.9, 24.4, 24.3, 24.2, 23.1, 22.3, 22.2, 21.9, 14.6. IR (Nujol, ν/cm^{-1}): 1745 (s), 1688 (s), 1578 (s), 1546 (s), 1515 (s), 1483 (s), 1315 (s), 1231 (s), 1168 (s), 1109 (s), 1054 (s), 1035 (s), 1021 (s). Anal. Calcd for $C_{39}H_{53}N_3O_2Pb$: C, 58.31; H, 6.66; N, 5.23. Found: C, 58.39; H, 6.54; N, 5.24.

[CH{(CH$_3$)$_2$CN-2,6-^{i}Pr$_2$C$_6$H$_3$}$_2$PbO^{s}Bu]. A suspension of KO^{s}Bu (0.085 g, 757 mmol in 3 mL of toluene) was added dropwise to a stirred solution of **1** (0.500 g, 757 mmol) in toluene (10 mL) at room temperature. The reaction mixture was stirred overnight. The deep-yellow solution was filtered through Celite, and the solvent was removed under vacuum. The resulting yellow solid was dissolved in the minimum amount of pentane (~7 mL) and stored at −30 °C overnight, yielding yellow crystals of (BDI)PbOsBu (0.441 g, 83%). ^{1}H NMR (toluene-d_8, 303 K): δ 7.17 (d, 2H, J = 7.5 Hz, *m*-*H*), 7.03 (t, 2H, J = 16.9 Hz, *p*-*H*),

(18) Sheldrick, G. M. *SHELXL-97, Program for the Refinement of Crystal Structures*; University of Göttingen: Göttingen, Germany, **1997**.

(19) The solution-phase chemistry of this compound is complex and is undergoing further studies to understand the variable-temperature NMR spectroscopic behavior.

(20) Maksic, Z. B.; Kovacevic, B. *J. Chem. Soc., Perkin Trans. 2* **1999**, 2623.

7.02 (d, 2H, J = 18.4 Hz, *m-H*), 4.60 (s, 1H, middle C*H*), 4.56 (m, 1H, OC*H*(CH_3)CH_2CH_3), 3.79 (hept, 1H, J = 6.9 Hz, C*H*Me_2), 3.77 (hept, 1H, J = 7.1 Hz, C*H*Me_2), 3.10 (septet, 2H, J = 6.8 Hz, C*H*Me_2), 1.64 (s, 3H, NC*Me*), 1.63 (s, 3H, NC*Me*), 1.47 (dd, 6H, J_1 = 6.5 Hz, J_2 = 4.8 Hz, CH*Me*$_2$), 1.21 (dd, 6H, J_1 = 6.8 Hz, J_2 = 1.7 Hz, CH*Me*$_2$), 1.15 (d, 6H, J = 6.8 Hz, CH*Me*$_2$), 1.12 (d, 6H, J = 6.8 Hz, CH*Me*$_2$), 0.78 (d, 3H, J = 6.0 Hz, OCH(C*H*$_3$)CH_2CH_3), 0.48 (t, 3H, J = 7.4 Hz, OCH(CH_3)CH_2C*H*$_3$). $^{13}C\{^1H\}$ NMR (C_6D_6, 303 K): δ 163.4 (N*C*Me), 144.7 (*ipso-C*), 142.8 and 141.6 (*o-C*), 125.8 (*p-C*), 123.4 and 123.3 (*m-C*), 99.1 (middle *C*H), 70.8 (O*C*(CH_3)CH_2-CH_3), 36.3 (OC(*C*H_3)CH_2CH_3), 27.9 (NC*Me*), 27.8 and 27.7 (*C*HMe_2), 26.0, 25.0, 24.2, and 23.7 (CH*Me*$_2$), 24.4 (OC(CH_3)-*C*H_2CH_3), 10.5 (OC(CH_3)CH_2*C*H_3). ^{207}Pb NMR (400 MHz, C_6D_6): δ 1542.8. IR (Nujol, ν/cm^{-1}): 3057, 1556 (s), 1516 (s), 1437 (s), 1251, 1171, 1100 (s), 1023 (s), 986, 961, 936, 917, 840, 791 (s), 750. IR (CCl_4, ν/cm^{-1}): 3059 (w), 2962, 2927, 2989, 2291 (w), 2004 (w), 1857 (w), 1550 (s), 1463, 1437, 1359, 1320, 1252 (s), 1217 (s), 1172. Anal. Calcd for $C_{33}H_{48}N_2O_3Pb$: C, 56.79; H, 7.22; N, 4.01. Found: C, 56.66; H, 7.08; N, 3.89.

[CH{(CH$_3$)$_2$CN-2,6-^{i}Pr$_2$C$_6$H$_3$}$_2$Pb(CO$_2$)O^{s}Pr] (9). 8 (101 mg, 0.145 mmol) was dissolved in toluene (8 mL) in a sealable ampule. The gas was evacuated, and CO_2 was added (0.220 mmol). The reaction mixture was cooled to −80 °C to give a yellow powder. ^{1}H NMR (C_6D_6, 303 K): δ 7.09 (s, br, 6H, Ar*H*), 4.78 (s, 1H, middle C*H*), 4.71 (sext, 1H, J = 6.21 Hz, OC*H*-(CH_3)CH_2CH_3), 3.30 (br, 4H, C*H*Me_2), 1.67 (m, 1H, OCH-(CH_3)CH_2CH_3), 1.62 (s, 6H, NC*Me*), 1.48 (m, 1H, OCH-(CH_3)CH_2CH_3), 1.26 (d, 12H, J_1 = 6.2 Hz, CH*Me*$_2$), 1.18 (d, 3H, J = 6.9 Hz, OCH(C*H*$_3$)CH_2CH_3), 1.11 (d, 12H, CH*Me*$_2$), 0.90 (t, 3H, J = 7.4 Hz, OCH(CH_3)CH_2C*H*$_3$). $^{13}C\{^1H\}$ NMR (C_6D_6, 303 K): δ 163.7 (N*C*Me), 160.7 (O*C*O$_2$), 142.4 (*ipso-C*), 127.7 and 127.5 (*o-C*), 126.5 (*p-C*), 124.4 and 124.0 (*m-C*), 103.2 (middle *C*H), 73.2 (O*C*(CH_3)CH_2CH_3), 29.3 (OC(*C*H_3)CH_2-CH_3), 27.8 (NC*Me*), 24.2 (*C*HMe_2), 24.1 (CH*Me*$_2$), 19.7 (OC(CH_3)*C*H_2CH_3), 9.8 (OC(CH_3)CH_2*C*H_3). ^{207}Pb NMR (400 MHz, C_6D_6): δ 810.3. IR (Nujol, ν/cm^{-1}): 3027, 2336 (w), 1940 (w), 1855 (w), 1800 (w), 1604, 1549 (s), 1260 (s), 1081 (s, br), 804 (s), 694 (s). IR (CCl_4, ν/cm^{-1}): 3723, 2693, 3621, 3590, 3063 (w), 2963, 2928, 2870, 2337 (s), 2005 (w), 1857 (w), 1645, 1550 (s), 1459, 1437, 1383, 1364, 1319, 1254 (s), 1217 (s), 1174. Note: traces of **8** were found in isolated solid-state samples of **9** (even crystallized samples), preventing acceptable elemental analysis.

Computational Details. All calculations were performed using the *Gaussian 03*, revision C.02, suite of programs using the B3LYP density functional theory and LanL2DZ pseudopotentials (and basis set).[15]

Acknowledgment. The authors are grateful for financial support from the EPSRC (Grant EP/E032575/1 to L.F.) and the University of Sussex.

Supporting Information Available: ORTEP diagram, crystallographic data, and selected bond lengths and angles for complex **8** and crystallographic data in CIF format for complexes **2**, **3**, **5**, **7**, and **8**. This material is available free of charge via the Internet at http://pubs.acs.org.